Photodissociation of an Internally Cold Beam of CH^+ Ions in a Cryogenic Storage Ring

A. P. O'Connor,[1] A. Becker,[1] K. Blaum,[1] C. Breitenfeldt,[1,2] S. George,[1] J. Göck,[1] M. Grieser,[1] F. Grussie,[1] E. A. Guerin,[1] R. von Hahn,[1] U. Hechtfischer,[1,*] P. Herwig,[1] J. Karthein,[1] C. Krantz,[1] H. Kreckel,[1,†] S. Lohmann,[1] C. Meyer,[1] P. M. Mishra,[1] O. Novotný,[1] R. Repnow,[1] S. Saurabh,[1] D. Schwalm,[1,3] K. Spruck,[4] S. Sunil Kumar,[1] S. Vogel,[1] and A. Wolf[1]

[1]*Max-Planck-Institut für Kernphysik, 69117 Heidelberg, Germany*
[2]*Institut für Physik, Ernst-Moritz-Arndt Universität, 17487 Greifswald, Germany*
[3]*Department of Particle Physics, Weizmann Institute of Science, Rehovot 76100, Israel*
[4]*Institut für Atom- und Molekülphysik, Universität Gießen, 35392 Gießen, Germany*

(Received 23 December 2015; published 17 March 2016)

We have studied the photodissociation of CH^+ in the Cryogenic Storage Ring at ambient temperatures below 10 K. Owing to the extremely high vacuum of the cryogenic environment, we were able to store CH^+ beams with a kinetic energy of ~60 keV for several minutes. Using a pulsed laser, we observed Feshbach-type near-threshold photodissociation resonances for the rotational levels $J = 0$–2 of CH^+, exclusively. In comparison to updated, state-of-the-art calculations, we find excellent agreement in the relative intensities of the resonances for a given J, and we can extract time-dependent level populations. Thus, we can monitor the spontaneous relaxation of CH^+ to its lowest rotational states and demonstrate the preparation of an internally cold beam of molecular ions.

DOI: 10.1103/PhysRevLett.116.113002

In 1941 Douglas and Herzberg attributed three interstellar absorption lines to the $^1\Pi \leftarrow {}^1\Sigma$ system of CH^+ [1]. This marked the first identification of a molecular ion in interstellar space. Today, more than 180 identified interstellar molecules bear witness to a rich chemical network operating even at the lowest temperatures and densities. In this framework CH^+ always played a special role [2], as there is no consistent explanation for its high abundance in the diffuse interstellar medium [3]. Given that CH^+ should be rapidly destroyed in collisions with ubiquitous hydrogen, and that no effective low-temperature formation route is known, the astrophysical puzzle turns out to be one of fundamental molecular reaction dynamics.

To study the potentials and states involved in low-temperature reactions, near-threshold photodissociation experiments probe the highest rovibrational states that are still bound. For CH^+, the photodissociation process

$$CH^+ + h\nu \rightarrow C^+(^2P_{1/2,3/2}) + H(^2S) \qquad (1)$$

has attracted attention as the reverse of the radiative association reaction, which has potential relevance in interstellar environments. While initial quantal calculations of this process found a strong energy dependence at low temperature [4], later work disagreed on the absolute rate coefficient [5]. Radiative association is considered too slow to be studied experimentally; therefore, theory relies on photodissociation studies to benchmark calculations.

Figure 1 shows the lowest CH^+ potentials based on *ab initio* calculations [6]. The Born-Oppenheimer potentials split at large distances into a ground term hydrogen atom and the two fine structure states of the C^+ ion, $C^+(^2P_{1/2})$ and $C^+(^2P_{3/2})$, which differ in energy by 63.4 cm^{-1}. Dipole-allowed transitions connect the $X^1\Sigma^+$ ground state with the first excited singlet state $A^1\Pi$. Asymptotically, the $A^1\Pi$ state correlates exclusively to the upper $C^+(^2P_{3/2})$ fine structure level. Therefore, if CH^+ is excited by ultraviolet radiation to energies just above the dissociation threshold, but below the energy of the $^2P_{3/2}$ level, the excited state has to couple nonadiabatically to the lower $^2P_{1/2}$ state before it can decay through predissociating resonances [7–9].

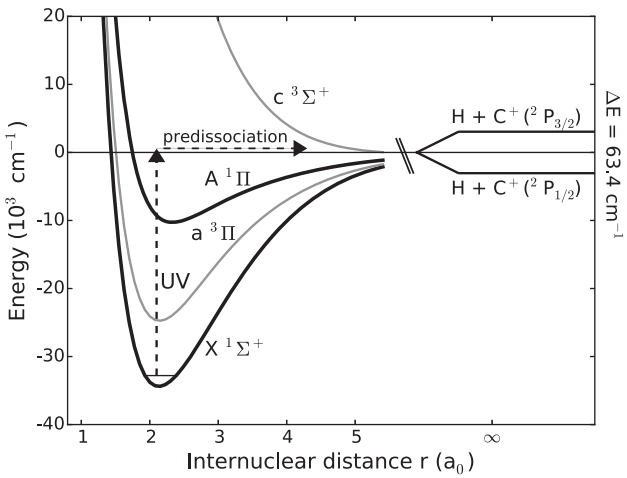

FIG. 1. Potential energy curves of the lowest electronic states of CH^+. The plot shows the Born-Oppenheimer potentials taken from Ref. [6] and the spin-orbit splitting at asymptotic distances (not to scale). The UV laser excitation and the subsequent predissociation process are indicated by dashed arrows.

Early photodissociation experiments with CH^+ employed the beam photofragmentation method (see Refs. [10,11] for reviews), using uncooled ion beams. This led to the detection of many shape resonances (quasibound rotational levels), while the Feshbach-type resonances originating from the lower J states remained elusive. The heavy-ion storage ring technique facilitated the preparation of rotationally relaxed (room temperature) ion beams, enabling the detection of the predissociation resonances of the lower lying CH^+ levels [12]. Subsequent multichannel cross section calculations were able to explain most of the structures in the experimental spectra [11], which represented a mixture of levels dominated by $J = 2$–6. Here we present photodissociation spectra measured in the Cryogenic Storage Ring (CSR), focusing on the lowest rotational states ($J = 0$–2) of CH^+. We combine experimental data with updated close-coupling calculations that allow us to quantify and analyze the populations of the individual quantum states inside the storage ring and demonstrate the preparation of a fast, internally cold CH^+ ion beam.

The CSR—located at the Max Planck Institute for Nuclear Physics in Heidelberg, Germany [13]—is the largest electrostatic storage ring project in the world [14]. The storage ring has a circumference of 35.1 m and features a nested vacuum system, to shield the inner experimental chambers from ambient air and radiation. The experimental chambers are cooled by a closed-circuit liquid helium refrigerator to temperatures below 10 K. At these temperatures the chamber walls act as a large cryosorbing surface, reducing the residual gas pressure to a minimum. All ion optical elements are fully electrostatic and allow for the storage of singly charged ion beams of almost arbitrary mass with kinetic energies up to 300 keV. The data presented here were taken during the first cold operation of the ring in July 2015.

The CH^+ ion beam was produced in a standard Penning ion source, accelerated to either 60 or 63 keV by an electrostatic platform, and injected into the CSR. During cryogenic operation the pressure inside the experimental chambers of the CSR is too low to be measured. Initial tests during the commissioning runs suggest that residual gas collisions are no longer limiting the beam lifetimes, but that small momentum diffusion effects may be responsible for the slow decay of the ion beam. While heavier molecular ions and clusters, that are less susceptible to small field perturbations, can be stored for several hours inside the CSR, the $1/e$ lifetime of the comparatively light CH^+ ions was on the order of ~200 s.

During storage the ions were irradiated by a pulsed (20 Hz repetition rate), tunable optical parametric oscillator (OPO) laser (Ekspla NT342b) at nominal wavelengths ranging from 301.6 to 303.4 nm (corresponding to ~33 160 and ~32 960 cm^{-1}, respectively). The laser was coupled into the experimental vacuum through sapphire viewports. The interaction zone was defined by two mirrors situated at a distance of 224 cm on opposite sides of the ion beam, such that the laser intersected the ion beam at a grazing angle of 3.4°. The laser beam was trailing the ion beam, and at an ion beam energy of 60 keV, the Doppler shift amounts to -103 cm^{-1}. The final wavelength scale was calibrated in comparison to the experimental data given in Ref. [11]. We corrected a systematic shift of 7.1 cm^{-1} with respect to the less precise factory calibration of our OPO laser system for all spectra, somewhat larger but on the same order as the laser linewidth (~4 cm^{-1} FWHM).

We also performed measurements at 63 keV beam energy, introducing an additional Doppler shift of ~2.5 cm^{-1}. This was necessary because the smallest step width of the OPO laser was ~5 cm^{-1}, which is comparable to the linewidth of the laser. We used the Doppler shift to repeat the measurements with a ~2.5 cm^{-1} offset. The spectra presented in this work result from the combination of both beam energies, normalized by a least-squares fit on a flat part of the spectra.

To detect the photodissociation events we used a microchannel plate in a straight extension downstream of the laser section, recording the neutral H atoms on an event-by-event basis. Owing to the small cross section of the photodissociation process (~10^{-20} cm^2 [9,12]) and the low output of the OPO laser at these wavelengths (<2 mJ), combined with the finite UV transmission of the cryogenic viewports and filters, we observed only roughly one event per 50 laser shots. For this reason we limited the storage time to 240 s, since it would have been too time-consuming to collect a consistent data set for significantly longer storage times.

Experimental spectra for six different storage time intervals are presented in Fig. 2, focusing exclusively on resonances associated with the states $J = 0$–2, as we expect all the population to accumulate in those states for storage times >30 s. The error bars reflect the counting statistics at the individual frequencies. We subtracted a small constant background caused by scattered UV laser light seen by the detector. This background was recorded in 5–25 s intervals at the end of each injection when we kicked out the ion beam but continued to fire the laser. The data were taken in the course of several days and the laser wavelength was stepped in ~1.9 s long intervals that were cycled such that in each injection a different wavelength would be sampled at the beginning of the storage time to average over systematic effects and slow drifts.

The experimental data were fitted by theoretical calculations (folded with a Gaussian laser linewidth of 4 cm^{-1} FWHM), yielding individual cross sections originating from the lowest rotational states of the $X^1\Sigma$ ground state. The fit parameters represent the level populations in the respective rotational states, given in the insets of Fig. 2. Since none of the states with $J > 2$ exhibit any resonances at the frequencies probed here, they can only be seen through their continuum contributions, which are identical and nearly constant for all of them. Consequently, we

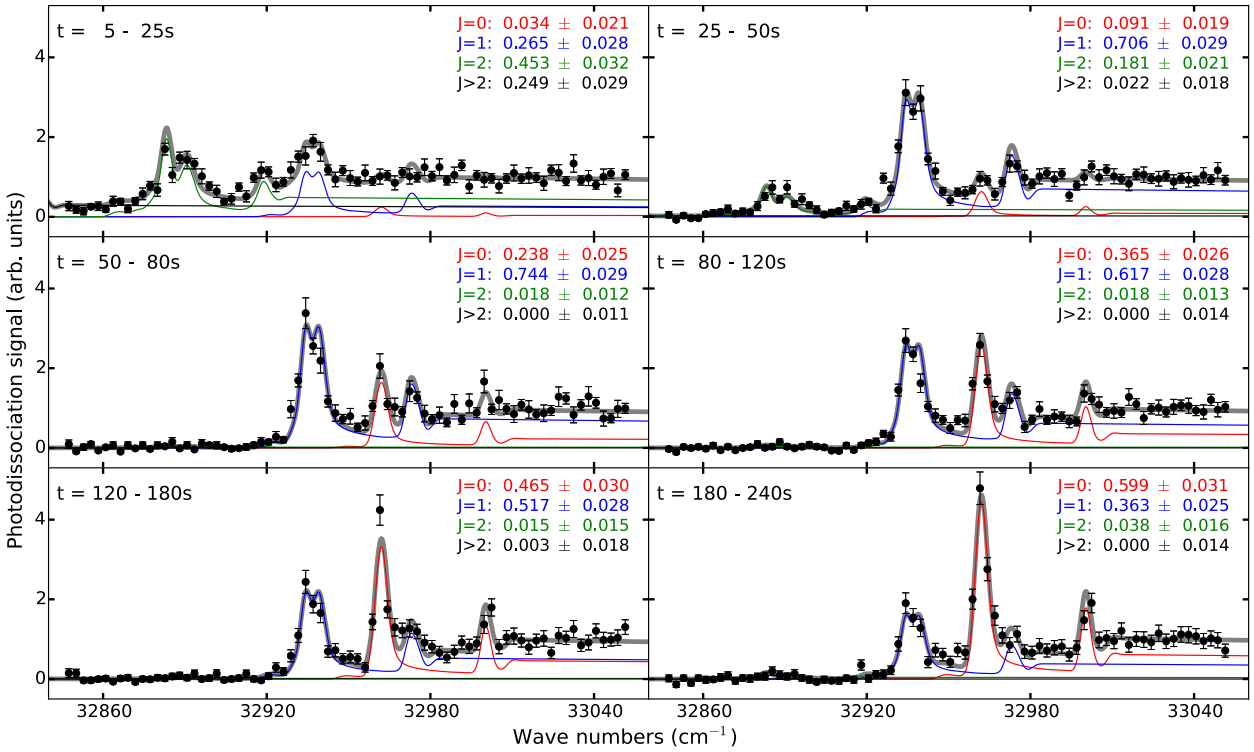

FIG. 2. Near-threshold photodissociation spectra of CH^+. The respective storage time intervals are given in the upper left-hand corner of the plots. The thick gray curve shows a fit of the calculated cross sections to the experimental data. The fit parameters represent the individual level populations in the lowest rotational states, which are given in the upper right-hand corner of each plot. The thin red, blue, and green lines show the cross sections for the individual states ($J = 0, 1, 2$) multiplied with their respective populations. All states with $J > 2$ are summed up into a single cross section (thin black line), as their continuum contributions in this wavelength range are identical and unspecific.

neither introduce uncertainties nor lose information by summing up all states with $J > 2$.

We computed updated photodissociation cross sections for the individual rotational states, employing the close-coupled framework applied to CH^+ by Williams and Freed in Ref. [9] and refined in Ref. [11]. The code calculates the multichannel scattering wave functions based on the potential matrix, which includes the Born-Oppenheimer potentials and nonadiabatic coupling terms (see Supplemental Material [15] and Ref. [11] for details).

The analysis of previous measurements [11] focused exclusively on the resonance behavior near threshold, at the expense of accurate relative cross sections for the individual J states. To this end, the potentials available at the time [17] were adjusted to obtain the best fit to the measured resonance structures. The $X^1\Sigma^+$ ground state potential had to be deepened by almost 3500 cm^{-1}, which made it incorrect for the description of the lower vibrational states [6]. Consequently, an analysis of the internal temperature of the ion ensemble was not attempted at the time; in fact, the relative strengths of the resonances were used as free parameters. However, while the unrealistic ground state potential shape was irrelevant for the understanding of the multichannel dynamics [15], it is relevant for this work, as we aim at an accurate description of the resonance shapes as well as the relative cross sections of the individual J states.

To generate new Born-Oppenheimer potentials with correct inner wells, we started from the improved *ab initio* potentials of Barinovs and van Hemert [6]. The calculations include relativistic corrections and core correlation, and already without adjustments these potentials lead to a photodissociation spectrum that is quite similar to the measured data [6], albeit without the exact match of the resonances that was reached by the procedure applied in Ref. [11]. Therefore, we fine-tuned the new potentials empirically to the previous room temperature experimental data [11], since at this temperature more J resonances can be used to match the potentials to the spectrum. We iteratively applied the close-coupling code to the adjusted potentials until they reproduced the room temperature data. Only small adaptations were required to achieve an excellent match [15], without the need to scale the individual J-state contributions. As a result, our new theoretical cross sections are based on more realistic potential shapes than our previous calculations, and we consider the relative strengths of the cross sections for different rotational states to be reliable. With the cryogenic

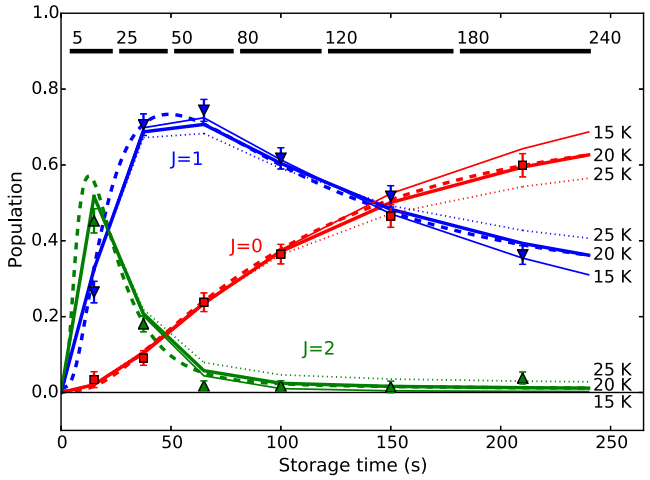

FIG. 3. Time-dependent CH^+ level populations. The markers with error bars result from the fits to the photodissociation data shown in Fig. 2. The experimental data are averaged over time intervals that vary in length from 20 to 60 s (shown by black bars at the top of the graph). The solid and dotted lines depict the outcome of a rate equation model that assumes a uniform blackbody radiation field at temperatures between 15 and 25 K (given at the individual curves). For fair comparison, the results have been averaged over the same time bins as the experimental data, taking into account the exponential decay of the ion beam. To show the influence of the time binning, the dashed curves represent the same data as the 20 K curves (thick solid lines), but without averaging. The initial rotational temperature of the injected ions is assumed to be >1000 K.

data, we can now verify in detail the calculated resonance intensities for the $J = 0$ and $J = 1$ states, which are very well reproduced by the updated theory.

Figure 2 shows the low-temperature experimental spectra as well as a fit with the theoretical cross sections and the individual J-state contributions. The populations of the rotational quantum states are the only remaining free parameters. The dependence of the state populations on the storage time are plotted in Fig. 3 together with the results of a simple rotational relaxation model based on the Einstein coefficients of the CH^+ rotational states. We assumed initial (ion source) temperatures between 1000 and 10 000 K and calculated the time-dependent rotational populations for a blackbody radiation field of 15, 20, and 25 K. To also cover high initial temperatures, we included $J = 0$–30 in the model. However, it turned out that the ion source temperature has little influence on the populations of $J = 0$–2 for storage times of more than 5 s, as long as the temperature exceeds 1000 K, which is a reasonable assumption for most standard discharge ion sources. The model neglects vibrational excitation (all vibrational states have lifetimes <1 s [18]) and the metastable $a^3\Pi$ state (lifetime 7 ± 1 s [19]) as their decay is independent from the slow rotational cooling that is the focus of the present work.

Since our analysis relies on the correct description of the rotational relaxation, we took great care to use accurate Einstein coefficients for the model. The ground state dipole moment of CH^+ has recently been calculated for precision Penning trap measurements to be 0.3505 e Å [20]. We recalculated the transition dipole moments for the lowest J states using very recent wave functions [21] and dipole functions [22], resulting in a value of 0.3507 e Å for $J =$ 0–2 (the rotational levels do not alter the wave function enough to make a significant difference). With this transition dipole moment and the known level energies (derived from rotational constants [23]) of 27.85 cm^{-1} for $J = 1$ and 83.53 cm^{-1} for $J = 2$, we obtain lifetimes of 156 s and 16.3 s, respectively. We estimate the Einstein coefficients to be accurate to within 1%.

We find that the rotational cooling of CH^+ inside the CSR can be described by an effective radiation field of approximately 20 K. While the nominal temperatures of the experimental vacuum chambers were measured to be <10K, the somewhat elevated effective temperature is not surprising, as there are several locations in the inner chambers—e.g., vacuum viewports and the injection section—where radiation from warmer parts can make it into the experimental chambers. Nevertheless, the resulting temperature is well below typical kinetic temperatures in interstellar clouds, and it would asymptotically lead to more than 70% population in $J = 0$. For small molecular ions with larger rotational constants (HD^+, HeH^+, etc.), we would expect almost exclusive population of $J = 0$ at long storage times. This would allow for storage ring experiments with ensembles of molecular ions in their ground rotational state. It should be mentioned in this context that the preparation of single rotationally cold molecular ions has been demonstrated previously in Penning traps [24,25].

Our results show that the complex multichannel process of CH^+ near-threshold photodissociation is well understood both experimentally and theoretically. The low rotational excitation realized in our experiment allows us to directly probe the relative intensities of different resonances for a given J and to characterize the C^+–H interaction in a specific fine structure level of C^+ and at the lowest relative angular momenta, which are particularly relevant to cold collisions. Our updated potentials precisely describe the nonadiabatic coupling leading to Feshbach resonances in the cold collision regime, while they retain the correct inner wells of the CH^+ system. Therefore, these potentials should be ideally suited for improved calculations on the C^++H radiative association process at interstellar temperatures. As the near-threshold resonances are responsible for a significant contribution to the radiative association rate, our results may help to shed light on the discrepancy between quantum calculations [4,5].

While our results do not offer a solution for the interstellar CH^+ puzzle yet, they show that reaction studies at true interstellar conditions are within our experimental capabilities now. The fact that the level populations of an infrared-active molecule like CH^+, stored in a cryogenic

ring, can be predicted by a simple rate model—effectively independent of the initial ion source temperature—is of outstanding importance for the emerging experimental program of cold molecular ion studies at electrostratic storage rings [14]. It also paves the way for state-selected merged beams experiments, including important processes like dissociative electron recombination and ion neutral reactions (e.g., $CH^+ + H \rightarrow C^+ + H_2$), which have attracted a lot of attention recently [26–29].

We thank Carl J. Williams for providing the close-coupling code. A. P. O., F. G., E. A. G., and H. K. were supported by the European Research Council under Grant Agreement No. StG 307163. D. S. acknowledges support by the Weizmann Institute through the Joseph Meyerhoff program. We thank Lutz Schweikhard for the loan of the OPO laser system. We are grateful to Stephan P. A. Sauer and Vladimír Špirko for providing accurate ground state wave functions and to Ğirts Barinovs and Marc C. van Hemert for their *ab initio* potentials. A. B., K. S., and S. S. K. were supported by the Deutsche Forschungsgemeinschaft (DFG) within the DFG Priority Program 1573 "Physics of the Interstellar Medium".

*Present address: Lumileds Germany GmbH, 52068 Aachen, Germany.

†Corresponding author.
holger.kreckel@mpi-hd.mpg.de

[1] A. E. Douglas and G. Herzberg, Astrophys. J. **94**, 381 (1941).
[2] J. H. Black and A. Dalgarno, Astrophys. J. **34**, 405 (1977).
[3] B. Godard, E. Falgarone, M. Gerin, D. C. Lis, M. De Luca, J. H. Black, J. R. Goicoechea, J. Cernicharo, D. A. Neufeld, K. M. Menten, and M. Emprechtinger, Astron. Astrophys. **540**, A87 (2012).
[4] M. M. Graff, J. T. Moseley, and E. Roueff, Astrophys. J. **269**, 796 (1983).
[5] Ğ. Barinovs and M. C. van Hemert, Astrophys. J. **636**, 923 (2006).
[6] Ğ. Barinovs and M. C. van Hemert, Chem. Phys. Lett. **399**, 406 (2004).
[7] M. M. Graff and J. T. Moseley, Chem. Phys. Lett. **105**, 163 (1984).
[8] M. M. Graff, J. T. Moseley, J. Durup, and E. Roueff, J. Chem. Phys. **78**, 2355 (1983).
[9] C. J. Williams and K. F. Freed, J. Chem. Phys. **85**, 2699 (1986).
[10] K. P. Kirby and E. F. van Dishoeck, Adv. At. Mol. Phys. **25**, 437 (1988).
[11] U. Hechtfischer, C. J. Williams, M. Lange, J. Linkemann, D. Schwalm, R. Wester, A. Wolf, and D. Zajfman, J. Chem. Phys. **117**, 8754 (2002).
[12] U. Hechtfischer, Z. Amitay, P. Forck, M. Lange, J. Linkemann, M. Schmitt, U. Schramm, D. Schwalm, R. Wester, D. Zajfman, and A. Wolf, Phys. Rev. Lett. **80**, 2809 (1998).
[13] R. von Hahn, F. Berg, K. Blaum, J. C. Lopez-Urrutia, F. Fellenberger, M. Froese, M. Grieser, C. Krantz, K.-U. Kühnel, M. Lange, S. Menk, F. Laux *et al.*, Nucl. Instrum. Methods Phys. Res., Sect. B **269**, 2871 (2011).
[14] H. T. Schmidt, Phys. Scr. **T166**, 014063 (2015).
[15] See Supplemental Material at http://link.aps.org/supplemental/10.1103/PhysRevLett.116.113002, which includes Ref. [16], for further information on the cross section calculations and the underlying potentials.
[16] P. G. Hajigeorgiou and R. J. Le Roy, J. Chem. Phys. **112**, 3949 (2000).
[17] M. Hanrath and S. D. Peyerimhoff (private communication).
[18] F. R. Ornellas and F. B. C. Machado, J. Chem. Phys. **84**, 1296 (1986).
[19] Z. Amitay, D. Zajfman, P. Forck, U. Hechtfischer, B. Seidel, M. Grieser, D. Habs, R. Repnow, D. Schwalm, and A. Wolf, Phys. Rev. A **54**, 4032 (1996).
[20] M. Cheng, J. M. Brown, P. Rosmus, R. Linguerri, N. Komiha, and E. G. Myers, Phys. Rev. A **75**, 012502 (2007).
[21] S. P. A. Sauer and V. Špirko, J. Chem. Phys. **138**, 024315 (2013).
[22] Z. Biglari, A. Shayesteh, and A. Maghari, Comput. Theor. Chem. **1047**, 22 (2014).
[23] A. Carrington and D. A. Ramsay, Phys. Scr. **25**, 272 (1982).
[24] J. K. Thompson, S. Rainville, and D. E. Pritchard, Nature (London) **430**, 58 (2004).
[25] B. J. Mount, M. Redshaw, and E. G. Myers, Phys. Rev. A **85**, 012519 (2012).
[26] R. Plasil, T. Mehner, P. Dohnal, T. Kotrik, J. Glosik, and D. Gerlich, Astrophys. J. **737**, 60 (2011).
[27] T. Grozdanov and R. McCarroll, Chem. Phys. Lett. **575**, 23 (2013).
[28] S. Bovino, T. Grassi, and F. A. Gianturco, J. Phys. Chem. A **119**, 11973 (2015).
[29] G. Werfelli, P. Halvick, P. Honvault, B. Kerkeni, and T. Stoecklin, J. Chem. Phys. **143**, 114304 (2015).